Microwave and Terahertz wave sensing with metamaterials

Hu Tao,[1] Emil A. Kadlec,[2] Andrew C. Strikwerda,[3] Kebin Fan,[1] Willie J. Padilla,[4] Richard D. Averitt,[3] Eric A. Shaner,[2*] and X. Zhang[1,]

[1]*Department of Mechanical Engineering, Boston University, Boston, MA 02215, USA*
[2]*Sandia National Laboratory, Albuquerque, NM 87185, USA*
[3]*Department of Physics, Boston University, Boston, MA 02215, USA*
[4]*Department of Physics, Boston College, Chestnut Hill, MA 02467, USA*

*eashane@sandia.gov
xinz@bu.edu

Abstract: We have designed, fabricated, and characterized metamaterial enhanced bimaterial cantilever pixels for far-infrared detection. Local heating due to absorption from split ring resonators (SRRs) incorporated directly onto the cantilever pixels leads to mechanical deflection which is readily detected with visible light. Highly responsive pixels have been fabricated for detection at 95 GHz and 693 GHz, demonstrating the frequency agility of our technique. We have obtained single pixel responsivities as high as 16,500 V/W and noise equivalent powers of 10^{-8} W/Hz$^{1/2}$ with these first-generation devices.

OCIS codes: (160.3918) Metamaterials; (040.2235) Detectors, Far infrared or terahertz; (050.6875) Three-dimensional fabrication; (300.6495) Spectroscopy, terahertz;

References and links

1. D. R. Smith, J. B. Pendry, and M. C. K. Wiltshire, "Metamaterials and Negative Refractive Index," *Science* **305**, 788 (2004).
2. D. Schurig, J. J. Mock, B. J. Justice, S. A. Cummer, J. B. Pendry, A. F. Starr, and D. R. Smith, "Metamaterial Electromagnetic Cloak at Microwave Frequencies," *Science* **314**, 977 (2006).
3. J. Valentine, J. Li, T. Zentgraf, G. Bartal, and X. Zhang, "An Optical Cloak Made of Dielectrics," *Nature Materials* **8**, 568 (2009).
4. J. B. Pendry, "Negative Refraction Makes a Perfect Lens," *Phys. Rev. Lett* **85**, 3966 (2000).
5. N. Fang, H. Lee, C. Sun, and X. Zhang, "Sub-Diffraction-Limited Optical Imaging with a Silver Superlens," *Science* **308**, 53 (2005).
6. H. Tao, W. J. Padilla, X. Zhang, R. D. Averitt "Recent Progress in Electromagnetic Metamaterial Devices for Terahertz Frequencies," *IEEE J. Sel. Top. Quan. Elec.* **17**, 92 (2011).
7. Bradley Ferguson and Xi-Cheng Zhang, "Materials for Terahertz Science and Technology," *Nature Materials* **1**, 26 (2002)
8. K. Sakai, *Terahertz Optoelectronics,* Berlin: Springer-Verlag (2005).
9. P.U. Jepsen, D. G. Cooke, M. Koch, "Terahertz spectroscopy and imaging – modern techniques and applications," Laser Photonics Rev. **5**, 124 (2011).
10. D. R. Smith, W. J. Padilla, D. C. Vier, S. C. Nemat-Nasser, and S. Schultz, "Composite Medium with Simultaneously Negative Permeability and Permittivity," *Phys. Rev. Lett.* **84**, 4184 (2000).
11. N. I. Landy, S. Sajuyigbe, J. J. Mock, D. R. Smith, and W. J. Padilla, "Perfect Metamaterial Absorber," *Phys. Rev. Lett.* **100**, 207402 (2008).
12. H. Tao, N. I. Landy, C. M. Bingham, X. Zhang, R. D. Averitt, and W. J. Padilla, "A Metamaterial Absorber for the Terahertz Regime: Design, Fabrication and Characterization," *Optics Express* **16**, 7181 (2008).
13. J. Hao, J. Wang, X. Liu, W. J. Padilla, L. Zhou, and M. Qiu, "High Performance Optical Absorber Based on a Plasmonic Metamaterial," *Appl. Phys. Lett.* **96**, 251104 (2010).
14. M. Tonouchi, "Cutting-edge Terahertz Technology," Nature Photonics **1**, 97 (2007).
15. F. Sizov and A. Rogalski, "THz Detectors," *Progress in Quantum Electronics* **32**, 278 (2010).
16. F. Sizov, V. Reva, A. Golenkov, and V. Zabudsky, "Uncooled Detectors Challenges for THz/sub THz Arrays Imaging," *Journal of Infrared, Millimeter and Terahertz Waves* **32**, DOI: 10.1007/s10762-011-9789-2 (2011).

#153512 - $15.00 USD Received 25 Aug 2011; revised 22 Sep 2011; accepted 22 Sep 2011; published 18 Oct 2011

17. H. Tao, C. M. Bingham, A. C. Strikwerda, D. Pilon, D. Shrekenhamer, N. I. Landy, K. Fan, X. Zhang, W. J. Padilla, and R. D. Averitt, "Highly Flexible Wide Angle of Incidence Terahertz Metamaterial Absorber: Design, Fabrication, and Characterization," Phys. Rev. B **79**, 125104 (2009).
18. B. Li, "Design and Simulation of an Uncooled Doulbe-Cantilever Microbolometer with the Potential for ~ mK NETD," *Sensors and Actuators A: Physical* **112**, 351 (2004).
19. K. C. Liddiard," Thin-film Resistance Bolometer IR Detectors," *Infrared Physics* **24**, 57 (1984).
20. Q. Zhang, Z. Miao, Z. Guo, F. Dong, Z. Xiong, X. Wu, D. Chen, C. Li, and B. Jiao, "Optical Readout Uncooled Infrared Imaging Detector Using Knife-edge Filter Operation," *Optoelectronics Letters* **3**, 119 (2007).
21. Y. Zhao, M. Mao, R. Horowitz, A. Majumdar, J. Varesi, P. Norton, and J. Kitching, "Optomechanical Uncooled Infrared Imaging System: Design, Microfabrication, and Performance," *Journal of Microelectromechanical Systems* **11**, 136 (2002).
22. X. Liu, T. Starr, A. F. Starr, and W. J. Padilla, "Infrared Spatial and Frequency Selective Metamaterial with Near-Unity Absorbance," Phys. Rev. Lett. **104**, 207403 (2010).

1. Introduction

Recently, engineered materials composed of designed inclusions exhibiting unique electromagnetic (EM) properties not readily occurring in nature have attracted extraordinary interest from a wide group of scientists working in optics, physics, engineering, and material science [1]. Since the first demonstration of negative refractive index using metamaterials (MMs), world-wide effort has spawned numerous research thrusts resulting in advances such as super lenses and invisibility cloaks [2-5]. Sub-wavelength metamaterial elements can be tailored to provide a specific EM response at virtually any desired frequency [6]. This is particularly an advantage in the THz portion of the spectrum where thin film semiconductor compatible absorber elements can impact applications such as chemical sensing and noninvasive real-time imaging [7-9].

As effective media, MMs can be characterized by a complex refractive index $n = n_1 + in_2$ where n_1 is related to the phase velocity and n_2 to losses [10]. A large fraction of MM research has focused on applications related to engineering n_1 (e.g. negative refractive index) while at the same time minimizing n_2 and the associated losses. However, manipulating the loss through judicious design of effective n_2 is advantageous for certain applications as demonstrated with recent work on perfect absorbers [11-13]. For example, designing a compact absorbing element can lead to enhanced functionality of EM detectors. This is of topic of significant interest for THz frequencies where there is a strong need to create sensitive low-cost detectors, especially in multi-pixel focal plane modalities.

Indeed, THz imaging has been a very active research area with significant potential for non-invasive imaging due to the fact that terahertz radiation is non-ionizing and can pass through many optically opaque materials such as clothing, cardboard, and ceramics [14]. At present, there are both coherent and incoherent detection approaches applied to these problems. Coherent detection techniques include heterodyne THz mixers and THz time domain spectroscopy (THz-TDS). Incoherent or direct detection systems including Golay Cells, pyroelectric detectors, plasmon detectors, Schottky diodes, and various thermal detectors, each have relative merits and limitations [15-16]. In this manuscript, we report on the development of an uncooled metamaterial enhanced THz detector with optical read-out. Through the incorporation of split ring resonators (SRRS) a strong resonant response is obtained that can be designed for specific frequencies of interest.

2. Metamaterial Enhanced Bimaterial Cantilever Pixel

The microcantilever-based THz detector employs thermally sensitive bi-material elements realized by MEMS technology, as shown in Figure 1(a). Two styles of detectors have been designed, fabricated, and characterized with operating frequency at 95 GHz and 693 GHz. The dimensions are shown in Figure 2. The detector pixels are comprised of three basic components: 1) a THz wave absorber consisting of a single gold (Au) SRR patterned on a silicon nitride (SiNx) thin film serving as the supporting pad; 2) bi-material cantilever

#153512 - $15.00 USD Received 25 Aug 2011; revised 22 Sep 2011; accepted 22 Sep 2011; published 18 Oct 2011

actuation legs composed of layers of SiNx and Au which have a large coefficient of thermal expansion (CTE) mismatch; 3) an optically reflective surface for visible light readout of the thermal deflection of the cantilevers due to the absorption of THz radiation. On resonance, the incident THz radiation drives a current in the metallic SRR resulting in ohmic heating. The primary heat flow path is through the supporting bi-material actuation legs. Due to the CTE mismatch between Au and SiNx, the temperature change of the legs results in mechanical deflection of the cantilever which is sensed by optical interrogation of the reflector pad.

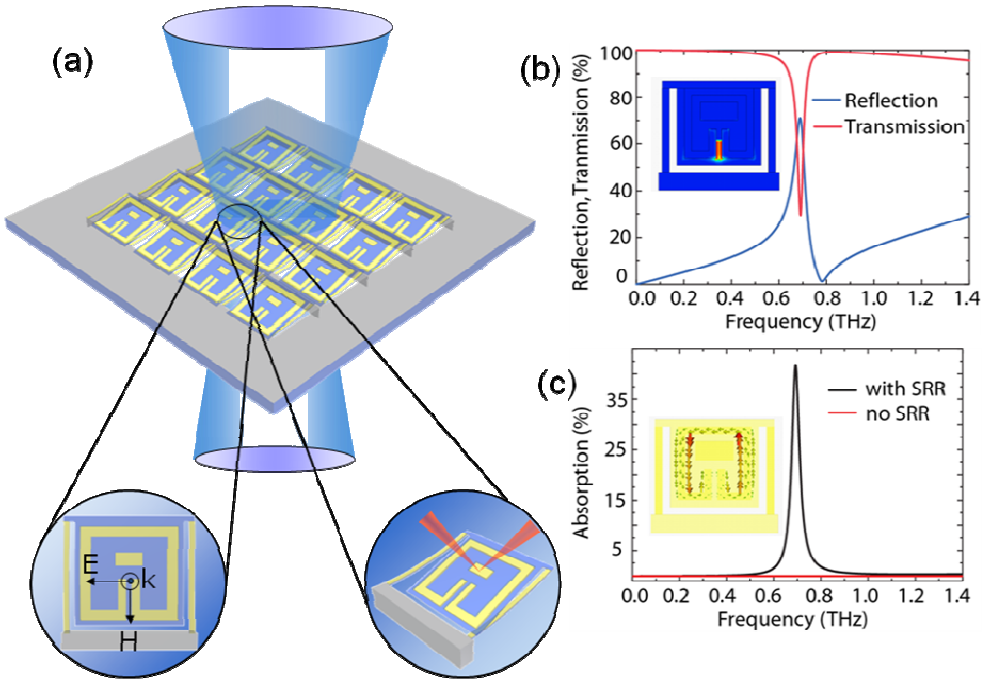

Fig. 1. Metamaterial enhanced terahertz detector using optical readout. (a). Schematic of the device showing the metamaterial cantilever array, an individual pixel, and reflective optical read-out. (b). Numerical simulation of the transmission reflection and transmission of the device. (Inset) Simulated electric field distribution on resonance (693GHz). (c). Numerical simulation of the absorption of the device with (black line) and without (red line) split ring resonators (SRRs). (Inset) Simulated surface current on resonance.

Figure 1(b) shows the simulation results of the field transmission (T) and reflection (R) of the metamaterial using CST STUDIO SUITE™ 2010. The absorptivity of the pixel could be then determined by the following equation: $A_{bs} = 1 - (T)^2 - (R)^2$. As shown in Figure 1(c), the absorption on resonance is approximately 40%, as opposed to nearly nothing with the bare SiNx pad. This absorption could potentially be further increased using a perfect absorber design though there could be a tradeoff with the increased thermal mass depending on the implementation [17].

3. Pixel Fabrication and Characterization

The THz detectors were fabricated using surface micromachining technology in a four-step process. First, a SiNx layer (500 nm) is deposited on a silicon substrate. The Cr/Au layer (10 nm/200 nm) defining the SRR absorbers, readout reflector, and cantilever legs is then fabricated using standard lithography and liftoff processes. Next, the SiNx layer is patterned using lithography and plasma etching to define the MM supporting membrane as well as the cantilever legs. Finally, the structures are released through backside KOH etching of the

#153512 - $15.00 USD Received 25 Aug 2011; revised 22 Sep 2011; accepted 22 Sep 2011; published 18 Oct 2011

underlying silicon substrate. The central image displayed with Figure 2 shows multiple pixels that were fabricated and released in this manner.

The THz photoresponse is detected by using a position sensitive photodetector (PSD) to measure the change in location of a reflected beam off of the optical pad of a pixel caused by the deflection of the cantilever. An electronically modulated frequency tripled YIG oscillator was used as the microwave source for the 95 GHz detector experiments. The THz source used for the 693 GHz measurements was an optically chopped CO_2 pumped far-infrared laser operating on a formic acid line. A 780 nm laser diode was focused onto the reflecting pad of the cantilever through a focusing objective and the back reflection was aligned to the PSD. The photoresponse was measured using a lock-in amplifier monitoring the output voltage of the PSD. For time-response measurements the signal was captured on an oscilloscope in place of the lock-in. While our fabrication naturally produces an array of cantilever pixels, in the following section we focus on characterizing the response of single pixels.

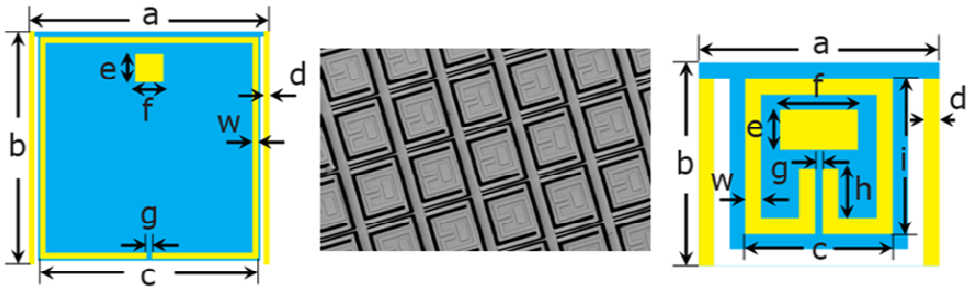

	a	b	c	d	e	f	g	h	i	w
95 GHz	435	415	395	10	50	50	10	—	—	10
690 GHz	80	67	49	5	13	26	2.5	16	51	5

All units are in microns.

Fig. 2. Dimensions of the metamaterial enhanced detectors resonant at 95 GHz and 693 GHz, respectively. The left (right) part of the figure shows the 95 GHz (693 GHz) pixel schematic while the center shows an SEM of a portion of the 693 GHz array.

4. Characterization of 95 GHz and 690 GHz Pixels

All measurements reported in this work were taken at room temperature and pressure. First, we consider the response of the 95 GHz detector. The spectral characteristics of the array were first verified using THz-TDS, as shown in Fig. 3 (inset). The dip in the transmission is associated with absorption (and reflection) of the SRRs. The resonance is centered at 95 GHz with a full-width at half max of 20 GHz. The photoresponse of the detector was characterized for both polarizations of the incident microwave radiation by stepping the operating frequency of the source over its full range from 60 GHz to 120 GHz. As shown in Figure 3, a strong resonant peak was observed at 95 GHz for the polarization having the electric field perpendicular to the SRR gap which drives the LC resonance. The photoresponse was significantly weaker for the orthogonal polarization with the electric field parallel to the gap.

#153512 - $15.00 USD Received 25 Aug 2011; revised 22 Sep 2011; accepted 22 Sep 2011; published 18 Oct 2011

In this case, the incident radiation does not couple to the resonance, which is the expected response for this particular SRR design.

After verifying the resonant response of the detector, the source was set to 95 GHz and the response of individual pixels were characterized as a function of incident power by attenuating the source with a voltage controlled attenuator. As shown in Figure 4, a nearly linear response of the detector was observed and follows the incident power reasonably well. A signal-to-noise ratio (SNR) of ~1,200 was obtained by measuring the peak signal (~380 mV) of the detector at the full incident power of 10 mW with a spot size of 1cm in diameter and noise floor of ~0.3 mV with no incident radiation. A responsivity of 16,500 V/W with a minimum NEP of $1x10^{-8}$ W/√Hz was obtained when considering the measurement bandwidth of the lock-in amplifier and the detector area. The temporal response of the detector, which is important for real-time imaging applications, was determined by monitoring the output signal of the PSD on an oscilloscope. The maximum operation frequency of the detector before signal roll off began was 15 Hz indicating a time constant of ~10 ms. The inset to Figure 4 shows the response at 5 Hz and 25 Hz showing that the response at 25Hz is still about 70% of the 5Hz response.

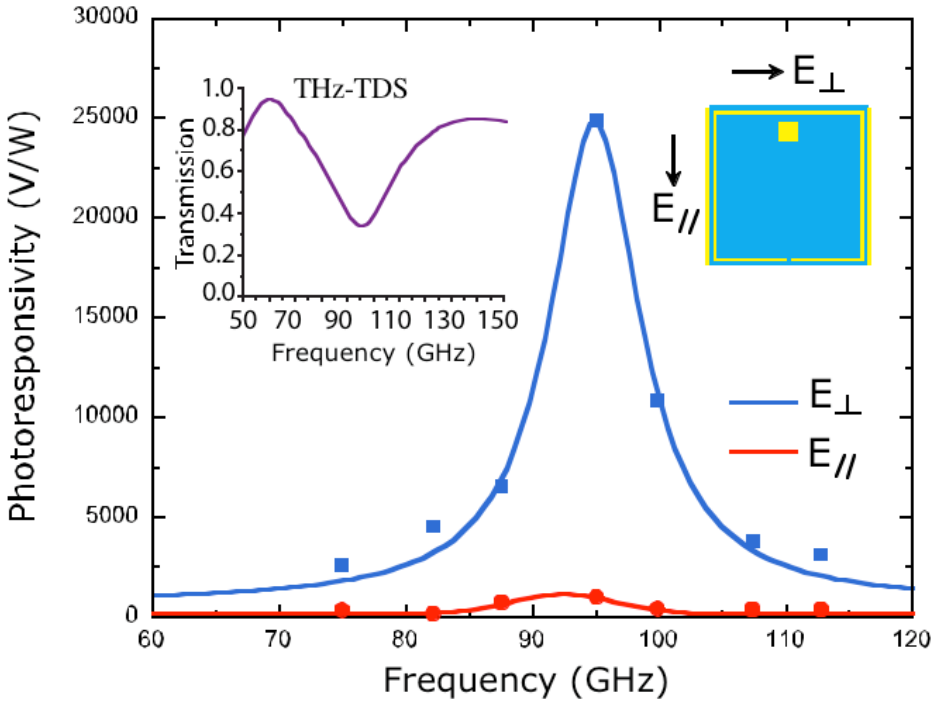

Fig. 3. Response of the 95 GHz detector as a function of frequency of the incident radiation at two polarizations. (Inset, left top) Transmission spectra of the detector characterized using Terahertz time-domain spectroscopy (THz-TDS). (Inset, left bottom) Zoom-in view of the detector response with the polarization of the THz electric field parallel to the SRR gap ($E_{\parallel}$). The response is two orders of magnitude smaller than the response with the polarization of the THz electric field perpendicular to the SRR gap ($E_{\perp}$). (Inset, right) Optical microscopy photo of one pixel of the 95 GHz detector with the two polarizations indicated.

The 693 GHz detector pixels were characterized with a similar setup using a far-infrared laser (FIRL) in place of the multiplier source. The resonant response of the 693 GHz detector was again pre-determined using THz-TDS as shown in the inset to Fig. 5(a). Both the polarization and the power of the FIRL source were controlled using a wire-grid polarizer pair. The FIRL beam was then focused using an off-axis parabolic mirror. The focused beam spot was measured using a pyrocam III beam imager in order to determine the peak intensity of the focused light as well as the beam diameter. A responsivity of 6,800 V/W with a minimum

#153512 - $15.00 USD Received 25 Aug 2011; revised 22 Sep 2011; accepted 22 Sep 2011; published 18 Oct 2011

NEP of 2.96×10^{-8} W/√Hz was experimentally obtained when considering the power incident on the single pixel. The temporal response (inset Fig. 5 (a) showing data at 8 Hz 15 Hz) of the 693 GHz detector shows a somewhat faster roll-off response in comparison to the 95 GHz pixel.

While the readout approach utilized could be significantly improved, we performed beam profiling measurements with the 693 GHz pixels in order to demonstrate the utility of our detectors, even at this stage, for THz beam diagnostics. In Fig. 5 (b), we show beam measurements taken using a single pixel while the beam was steered along both axes. To capture the beam along the y-axis, the focusing paraboloid was simply translated. In a similar way, the x-axis data was captured by rotating the focusing optic. The result was a Gaussian profile similar to that measured with the commercial beam imager. While this is by no means an ideal technique for characterizing the beam, it demonstrates that these relatively simple detector elements can immediately find lab applications should an appropriate multi-pixel readout scheme be implemented.

5. Discussion and Conclusions

It is worth mentioning that the performance of the metamaterial resonant detectors could be significantly improved based on the fact that our characterization was conducted at room temperature and pressure. The 95 GHz and 693 GHz pixels have similar noise which mainly comes from the optical readout system. The noise could be further reduced by using a more stable read-out laser, a higher sensitivity PSD, and further reducing the environmental vibration. Alternative signal addressing methods such as capacitive or resistive readouts could also be implemented [18-19]. Significant improvements in the thermal engineering should also improve the NEP. Preliminary estimates suggest a reduction of the NEP to 10^{-10} W/√Hz (and perhaps lower) is possible with additional engineering effort. In its present form using the experimental setup described in this paper and sub-wavelength pixels, the minimum power detectable in a diffraction limited spot is approximately 1 μW.

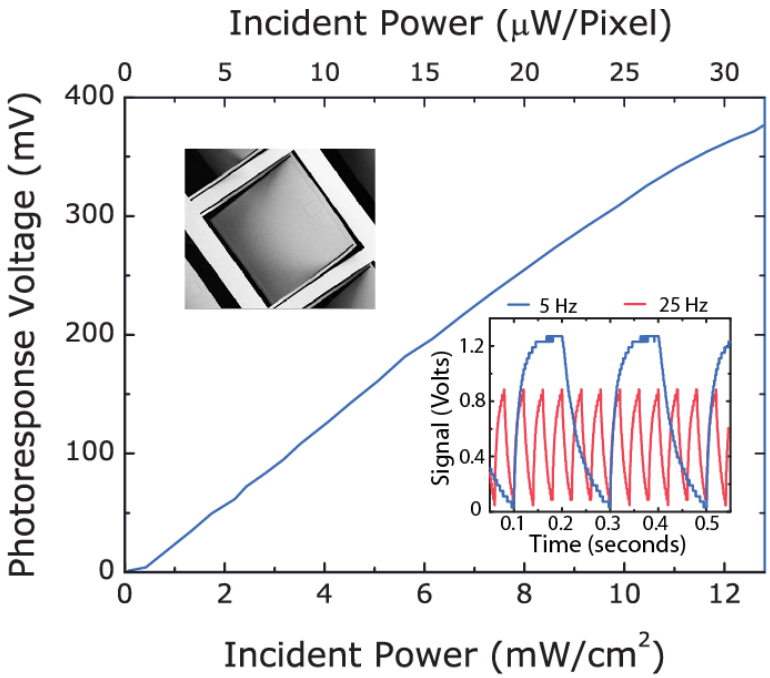

Fig. 4. Photoresponse of the 95 GHz pixel as a function of incident power. (Inset, left) SEM photo of one pixel. (Inset, right) Oscilloscope observed temporal response of the 95 GHz at 5 Hz (blue) and 25 Hz (red), respectively.

#153512 - $15.00 USD Received 25 Aug 2011; revised 22 Sep 2011; accepted 22 Sep 2011; published 18 Oct 2011

Our metamaterial cantilever detectors are naturally fabricated in array form and are therefore suitable for real-time 2D imaging by simultaneously measuring the deflection of all of the pixels using, for example, a visible CCD/CMOS camera to obtain an intensity map for parallel pixel readout [20-21]. Furthermore, it is possible to combine multiple SRRs with different resonant frequencies into a super pixel, thus enabling frequency-sensitive THz imaging/spectroscopy with a "multicolor" THz illumination source [6]. The optimal design of THz focal plane imaging detector will also need to consider pixel size for particular imaging needs such as speed and sensitivity. For example, the MM unit cells are typically $\lambda/5 \sim \lambda/10$ in size. One may desire to have multiple MM SRRs constructed on a sensing pixel element that is matched to the optics of the overall system for optimum response [22].

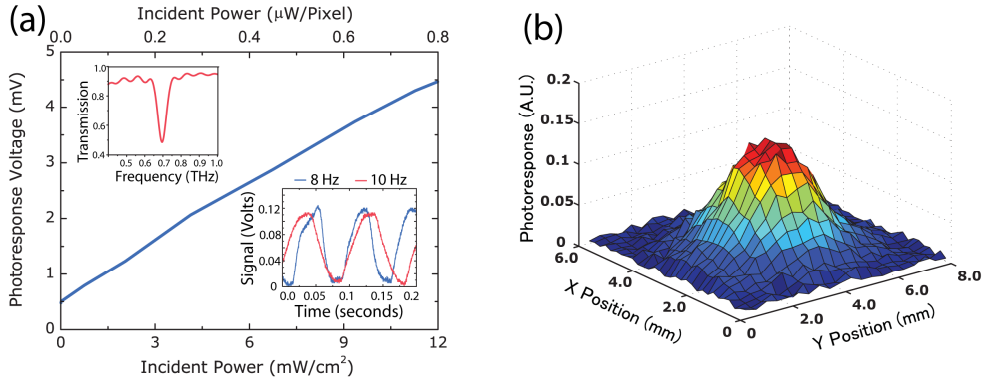

Fig. 5. Photoresponse of the 693 GHz pixel. (a). Response of the detector as a function of incident power. The non-zero intercept results from residual vibrations. (Inset, left) Oscilloscope observed temporal responses of the 95 GHz at 8 Hz (blue) and 10 Hz (red), respectively. (Inset, right) THz-TDS characterized transmission spectrum of the detector showing a resonance at ~ 693 GHz. (b). Image of the incident THz beam profile using the metamaterial enhanced THz detector.

In summary, we have developed metamaterial enhanced resonant detectors with a simple fabrication process for active THz sensing and detection applications. While we demonstrated detection at 95 GHz and 693 GHz, in principle this approach can be applied to other unconventional wavelengths where nature does not provide us with appropriate material resonances amenable to integration with thermal detection platforms. The implementation of low cost thin film THz absorbers could enable rapid progress in extending the many benefits of uncooled thermal imaging devices to the THz portion of the spectrum.

6. Acknowledgements

We acknowledge partial support from NSF under Contract No. ECCS 0802036, and AFOSR under Contract No. FA9550-09-1- 0708, and DARPA under Contract No. HR0011-08-1-0044. Sandia National Laboratories is a multi-program laboratory managed and operated by Sandia Corporation, a wholly owned subsidiary of Lockheed Martin Corporation, for the U.S. Department of Energy's National Nuclear Security Administration under contract DE-AC04-94AL85000. The authors would like to thank the Photonics Center at Boston University for all the technical support throughout the course of this research.

#153512 - $15.00 USD Received 25 Aug 2011; revised 22 Sep 2011; accepted 22 Sep 2011; published 18 Oct 2011